

ESCA Characterization of Perfluoroalkylene-Linked Polyquinolines

David T. Clark and Hugh S. Munro

Department of Chemistry, University of Durham, Durham City, DH1 3LE, England

Antonino Recca*

Istituto di Chimica, Facoltà di Ingegneria, 95125 Catania, Italy

John K. Stille

Department of Chemistry, Colorado State University, Fort Collins, Colorado 80523.

Received August 8, 1983

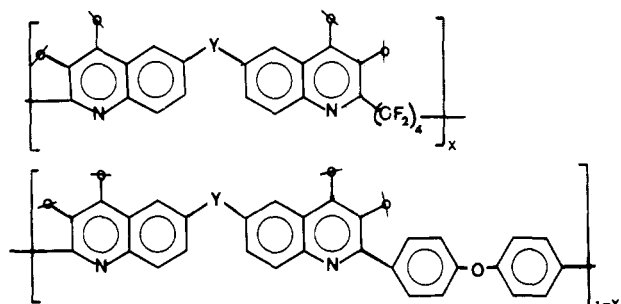
ABSTRACT: The ESCA characterization of some perfluoroalkylene-linked polyquinolines and a related model compound has been carried out. The results indicate a sufficient correspondence between the ESCA analysis and the predicted bulk compositions.

Introduction

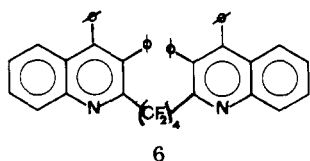
In the past few years there has been increasing interest in the synthesis of high molecular weight polyquinolines.¹⁻⁴ These polymers show excellent thermal stability,¹⁻⁵ but their processability is often quite limited because of the high T_g 's and, in some cases, the low solubility exhibited by these polymers.

Recently, in an effort to increase the processability of these polyquinolines, fluoromethylene groups have been successfully incorporated into the chain.⁶ In fact, a small percentage of perfluorobutylene groups in the polyquinoline chain was sufficient to decrease the T_g significantly while still allowing increasing desirable solution, film, and mechanical properties as well as thermal stability.

Unfortunately, the exact percentage of perfluoroalkylene groups introduced in the chains could not be determined for polymers containing a very low percentage of such groups ($\sim 5\%$).⁶ In fact, in these cases the fluorine analyses showed marked differences between the experimental and calculated values. Electron spectroscopy for chemical analysis (ESCA) has been shown to be a technique of prime importance in the characterization of polymer surfaces⁷⁻¹⁰ and has been successfully applied to the study of a wide range of fluorinated materials.⁷⁻¹⁰ Consequently, we have employed ESCA to investigate the surface aspects of the fluorinated polyquinolines 1-5 and a related model compound 6.



- 1, $x = 1$, $Y = O$
- 2, $x = 0.25$, $Y = O$
- 3, $x = 0.05$, $Y = O$
- 4, $x = 0$, $Y = O$
- 5, $x = 0.05$, $Y = \text{nil}$



Results and Discussion

The ESCA spectra displayed in Figure 1 reveal the typical C_{1s} , O_{1s} , N_{1s} , and F_{1s} core levels obtained for polymers 1, 2, and 4. The C_{1s} envelope for polymer 1 shows two prominent photoionization peaks centred at 285.0 and 290.9 eV. The former arises from carbon not bonded to nitrogen or fluorine, and the latter is indicative of the CF_2 groups present. The shoulder to the high binding energy side of the peak at 285.0 eV arises from a combination of C-N and C- CF_2 functionalities. The region centered at 290.9 eV also encompasses contributions from the $\pi-\pi^*$ shake-up satellites diagnostic of the aromatic ring systems present in the polymer. The contribution from the shake-up satellites is more evident on examining the C_{1s} envelope for the non-fluorine-containing homopolymer (4). All the systems studied show C_{1s} features similar to those described for polymer 1.

The binding energies for the N_{1s} , F_{1s} , and O_{1s} levels displayed in Figure 1 are consistent with those expected from the structural formula.⁷⁻⁹

The main interest in this work has been the determination of the relative N_{1s}/C_{1s} , O_{1s}/C_{1s} , and F_{1s}/C_{1s} area ratios and hence on inclusion of the appropriate instrument sensitivity factors for the stoichiometries. The relevant data are collected in Table I.

It is evident from the results for the O_{1s}/C_{1s} ratios that there is more oxygen present in the surface than predicted from the polymer repeat units. However, in all cases a small amount of surface contamination is present as is evident from the detection of an Si_{2p} signal (Figure 1).

Only in the case of polymer 3 (5% copolymer) was it possible to cast a good film due to the lower viscosity of the other polymers. On examining the appropriate core levels as a function of increasing take-off angle, one finds a concomitant increase in the Si_{2p}/C_{1s} ratio. This confirms the presence of the contaminant in the outermost regions of the sample. The low intensity of the Si_{2p} signal suggests a coverage for an overlayer thickness of ~ 2 Å. As a typical monolayer thickness is ~ 5 Å, the preliminary analysis suggests only a partial monolayer coverage.

The effect of this overlayer will be to attenuate the signals arising from the core levels of the pure polymer, as suggested by the data in Table I.

Previous studies have suggested and our experiments confirm (see Experimental Section) that the structure of the contaminant silicone material resembles poly(dimethylsiloxane), $(Si(CH_3)_2-O)_n$, and it is possible to model the effect of the patched overlayer within a substrate overlayer framework. (Model calculations rapidly establish that the contaminant overlayer is substantially less than

Table I

polymer	O_{1s}/C_{1s}			N_{1s}/C_{1s}			F_{1s}/C_{1s}		
	bulk calcd	exptl ^a	calcd extent % of coverage	bulk calcd	exptl ^a	calcd 5-Å overlayer	bulk calcd	exptl ^a	calcd 5-Å overlayer
1	0.022	0.045	10	0.043	0.032	0.042	0.17	0.13	0.17
2	0.034	0.075	20	0.038	0.026	0.035	0.038	0.036	0.035
3	0.036	0.088	25	0.037	0.033	0.034	0.0075	0.004	0.0065
4	0.037	0.064	13	0.037	0.037	0.035			
5	0.017	0.054	3	0.037	0.029	0.037	0.0075	0.004	0.0073
6		0.059	27	0.043	0.020	0.039	0.17	0.005	0.15

^a Obtained by taking into account the following instrument sensitivity factors: $O_{1s}/C_{1s} = 0.63$; $N_{1s}/C_{1s} = 0.736$; $F_{1s}/C_{1s} = 0.52$.

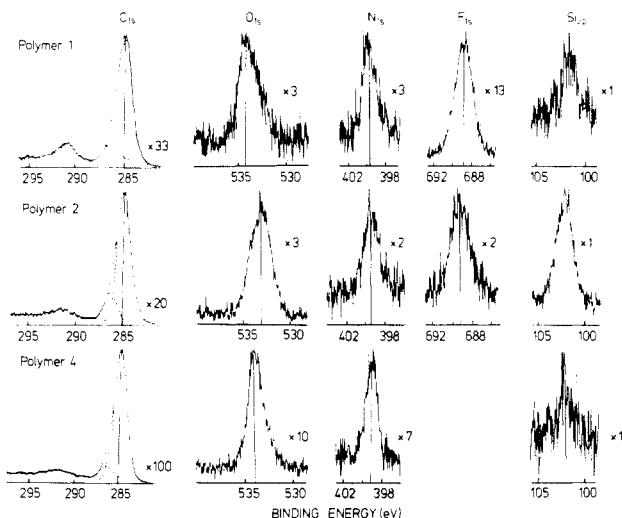


Figure 1. C_{1s} , O_{1s} , N_{1s} , F_{1s} , and Si_{2p} peaks for polymers 1, 2, and 4.

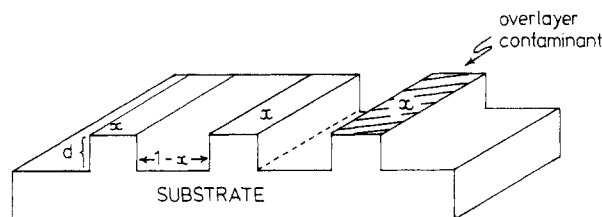


Figure 2. Patched overlayer coverage x at the surface.

a monolayer in all cases.) A schematic of the patched overlayer employed is displayed in Figure 2. The intensity of a given core level in the overlayer is

$$I_0 = K_1(1 - e^{-d/\lambda \cos \vartheta})$$

where K_1 encompasses the number average of atoms sampled, ionization cross section, instrumental transmission, etc., d is the depth, λ is the mean free path of the photoemitted electron, and ϑ is the electron take-off angle.⁷⁻⁹

The corresponding intensity for the substrate below the overlayer is

$$I_s = K_2(e^{-d/\lambda \cos \vartheta})$$

Thus the total signal intensity for a specific core level may be represented by

$$I_t = K_1x(1 - e^{-d/\lambda \cos \vartheta}) + K_2x(e^{-d/\lambda \cos \vartheta}) + K_2(1 - x) \quad (1)$$

where x is the extent of coverage of the overlayer.

Using the experimental O_{1s}/C_{1s} intensity ratio, taking the depth of the overlayer as 5 Å, and employing eq 1, it is possible to define x .

Subsequently the N_{1s}/C_{1s} and F_{1s}/C_{1s} intensity ratios for the pure polymer may be calculated, and the relevant results are displayed in Table I. Using this model, one

obtains a good agreement between the ESCA surface analysis (5-Å patched overlayer) and that calculated for the bulk polymers.

The data indicate a remarkably low level of surface contamination for these materials. As discussed above, the bulk analysis for fluorine showed marked differences between the experimental and predicted values for the polymers containing a low percentage of fluoromethylene groups. We have previously indicated that quantitative microanalysis of fluoro polymers by potassium fusion is very difficult and in the case of polymers containing ~1% fluorine, the errors could be very substantial.⁷⁻⁹

The close correspondence between the ESCA analysis which involves two independent analyses (based on C:F and C:N) and the predicted bulk compositions is only consistent with a random surface structure in which ESCA statistically samples the repeat units.

This is of interest since the repeat units are of a dimension commensurate with the typical electron mean free paths so that specific orientation effects would probably have been readily apparent from the ESCA data.

Unfortunately it is not possible to determine the percentage of CF_2 groups from the C_{1s} envelopes as a direct comparison to the F_{1s}/C_{1s} ratios due to the superposition of the CF_2 and shake-up peaks. However, from polymer 4 it is known that the shake-up intensity is ~6% of the total C_{1s} envelope. The expected contribution from CF_2 moieties in polymer 1 as determined from the repeat unit is ~8%, giving rise to a total area for the 291.0-eV region of 14%. This is in good agreement with the experimentally determined area of ~13%.

Experimental Section

Compounds 1-6 were prepared by the procedure already described in the literature.⁶

The ESCA spectra were run on an AEI ES300 electron spectrometer using a Mg $K\alpha_{1,2}$ X-ray source operated in a fixed retardation ratio mode. Spectra were analyzed using a Du Pont 310 curve resolver. Binding energies were referenced to the C-H level at 285.0 eV.

The samples were studied as powders except in the case of polymer 3, which was studied as a film.

The most likely source of silicone contamination is from grease used in the glassware involved in the synthetic procedures.

The level of silicone present (i.e., submonolayer) means that ESCA is the only technique for its direct detection and quantification. Our studies of the core level spectra for a thin film of conventional laboratory silicone grease confirms the model described in the previous section.

Acknowledgment. We gratefully acknowledge support of this research by NATO and the Italian CNR.

Registry No. 1, 80641-07-2; 2, 80641-04-9; 3, 80652-32-0; 6, 80640-60-4.

References and Notes

- (1) For a review, see: Stille, J. K. *Macromolecules* **1981**, *14*, 870.
- (2) Stille, J. K.; Harris, R. M.; Padaki, S. M. *Macromolecules* **1981**,

- 14, 486.
 (3) Sybert, P. D.; Beever, W. H.; Stille, J. K. *Macromolecules* 1981, 14, 493.
 (4) Beever, W. H.; Stille, J. K. *J. Polym. Sci., Polym. Symp.* 1978, No. 65, 41.
 (5) Wrasidlo, W.; Harris, S. O.; Wolfe, J. F.; Katto, J. F.; Stille, J. K. *Macromolecules* 1976, 9, 512.
 (6) Bottino, F. A.; Mamo, A.; Recca, A.; Droske, J. P.; Stille, J. K. *Macromolecules* 1982, 15, 227.

- (7) Clark, D. T. In "Electron Emission Spectroscopy"; Dekeyser, W., Reidel, D., Eds; D. Reidel Publishing Co.: Dordrecht, Holland, 1973; p 373.
 (8) Clark, D. T. In "Electronic Structure of Polymers and Molecular Crystals"; Ladik, J., Andre, J. M., Eds; Plenum Press: New York, 1975.
 (9) Clark, D. T. In "Advances in Polymer Science"; Springer-Verlag: Berlin, 1977.
 (10) Clark, D. T. *Pure Appl. Chem.* 1982, 54, 415.

Notes

Photopolymerization in Cholesteric Mesophases

PAUL J. SHANNON

Armstrong World Industries Inc., Research and Development, Lancaster, Pennsylvania 17604.
 Received June 27, 1983

We have been interested in the synthesis of polymeric liquid crystals that exhibit the optical properties of low molar mass cholesteric liquid crystals.¹ The early work of Liebert and Strzelecki² indicated that the cholesteric structure of twisted nematic phase could be "frozen-in" by rapid polymerization in the presence of high amounts of cross-linkers. Similarly, lyotropic cholesteric mesophases consisting of poly(γ -butyl L-glutamate) and triethylene glycol dimethacrylate have been photopolymerized without destruction of the cholesteric optical properties.³ Ringsdorf et al.⁴ demonstrated that cross-linking was not necessary in order to maintain cholesteric properties in a polymer. Through use of the concept of flexible spacer groups to decouple the mesogenic units from the restrictions of the main polymer chain, they found a 1:1 methacrylate copolymer consisting of cholesteryl esters with spacer groups of different lengths that exhibited cholesteric properties. Polymers exhibiting cholesteric properties also were obtained by copolymerization of nematic monomers with small amounts of chiral mesogenic monomers.⁵ Extending the idea of flexible spacer groups, Finkelmann and Rehage⁶⁻⁸ prepared several cholesteric polysiloxanes by using cholesteric esters as the chiral component in formation of twisted nematic phases. The same group also demonstrated that polymerization of chiral monomers that normally do not exhibit a liquid crystalline state can give homopolymers that exhibit cholesteric properties.⁹ Recently, thermotropic polymers based on derivatives of (2-hydroxypropyl)cellulose also have been shown to exhibit cholesteric optical properties.¹⁰⁻¹³

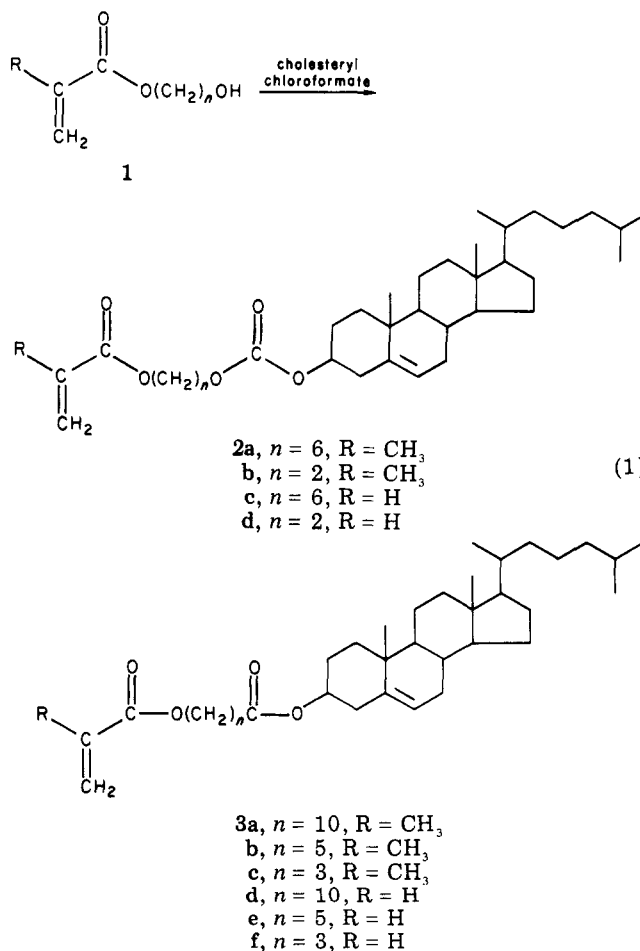
With one notable exception,⁴ monomers consisting of only cholesteryl ester mesogens, with or without flexible spacer groups, have failed to give polymers that exhibit cholesteric properties. In all cases the smectic structures have dominated the liquid crystalline phase of the polymers.¹⁴⁻¹⁸ Polymerization of mesogenic monomers stabilizes the liquid crystalline state, and the polymers exhibit a higher degree of order than the monomers.⁹ To circumvent the preference for smectic structures in polymers containing cholesteryl esters mesogens, polymerizations have been initiated in the cholesteric mesophases of the monomers. However, in all cases that do not involve extensive cross-linking, phase separation has resulted in amorphous or smectic polymers.¹⁹

We report here that cholesteric liquid crystalline monomers of structure 2 and 3, in combination with suitable

photoinitiators, undergo efficient photopolymerization to "freeze-in" the planar texture characteristic of low molar mass cholesteric liquid crystals.

Results and Discussion

The synthesis and phase transitions of the cholesteryl esters 3 have been described.²⁰ Monomers with cholesteryl carbonate moieties (2) were prepared by acylation of hydroxyalkyl acrylates or hydroxyalkyl methacrylates with cholesteryl chloroformate (eq 1). The phase transitions and spectral data for monomers 2 are listed in the Experimental Section.



Cholesteric mesophases typically are characterized by their ability to reflect light selectively in the infrared, visible, and ultraviolet regions. The wavelength of maximum reflection (λ_R) is related directly to the helical pitch (p) and the mean index of refraction (\bar{n}) of the cholesteric mesophase by $\lambda_R = \bar{n}p$.¹ The pitch may be quite sensitive